Brush-Induced Orientation of Collagen Fibers in Layer-by-Layer Nanofilms: A Simple Method for the Development of Human Muscle Fibers

Muhammad Haseeb Iqbal, Jeanne Rosine Faratiana, Emeline Pradel, Varvara Gribova, Kamel Mamchaoui, Catherine Coirault, Florent Meyer, Fouzia Boulmedais

Brush-Induced Orientation of Collagen Fibers in Layer-by-Layer Nanofilms: A Simple Method for the Development of Human Muscle Fibers

*Muhammad Haseeb Iqbal §, Faratiana Jeanne Rosine Revana §, Emeline Pradel §, Varvara Gribova £ †, Kamel Mamchaoui #, Catherine Coirault #, Florent Meyer £ †, and Fouzia Boulmedais §**

§ Université de Strasbourg, CNRS, Institut Charles Sadron, UPR 22, Strasbourg Cedex 2, 67034, France

£ Centre de Recherche en Biomédecine de Strasbourg, Institut National de la Santé et de la Recherche Médicale, UMR 1121, Biomatériaux et Bioingénierie, Strasbourg Cedex, 67085, France

† Université de Strasbourg, Faculté de Chirurgie Dentaire, Strasbourg, 67000, France

Sorbonne Université, INSERM UMRS 974, Centre for Research in Myology, Batiment Babinski, GH Pitié-Salpêtrière 47 bd de l'Hôpital, F-75013 Paris, France

*Email: fouzia.boulmedais@ics-cnrs.unistra.fr

KEYWORDS: Orientation, nano-patterning, multilayers, polyelectrolyte, myogenesis

ABSTRACT

The engineering of skeletal muscle tissue, a highly organized structure of myotubes, is promising for the treatment of muscle injuries and muscle diseases, for replacement or pharmacology research. Muscle tissue development involves differentiation of myoblasts into myotubes with parallel orientation, to ultimately form aligned myofibers, which is challenging to achieve on flat surfaces. In this work, we designed hydrogen-bonded tannic acid/collagen layer-by-layer (TA/COL LbL) nanofilms using a simple brushing method to address this issue. In comparison to films obtained by the dipping, brushed TA/COL films showed oriented COL fibers of 60 nm diameter along the brushing direction. Built at acidic pH due to COL solubility, TA/COL films released TA in physiological conditions with a minor loss of thickness. After characterization of COL fibers orientation, human myoblasts (C25CL48) were seeded on the oriented TA/COL film, ended by COL. After 12 days in a differentiation medium without any other supplement, human myoblasts were able to align on brushed TA/COL films and to differentiate into long aligned myotubes (from hundreds of nm up to 1.7 mm length) thanks to two distinct properties: (i) the orientation of COL fibers guiding myoblasts alignment, and (ii) the TA release favoring the differentiation. This simple and potent brushing process allows the development of anisotropic tissues *in vitro* which can be used for studies of drug discovery and screening or the replacement of damaged tissue.

Introduction

Musculoskeletal tissues are one of the most important components of the human body representing around 40% of adult body mass. Containing thousands of muscle fibers bundled together into an aligned parallel organization, their pivotal role is to perform routine voluntary locomotion by creating forces that are then transmitted by tendons towards the skeleton.[1] Muscle injuries are commonly caused by contusions during sports, accidental trauma, age-related wear *etc*.[2] Since the development of collagen-coated substrate to culture avian myotubes,[3] extensive research has been carried out to regenerate skeletal muscle tissue *in vitro* for the treatment of muscle injuries or diseases, such as muscular dystrophies or paralysis. Muscle development involves differentiation of myoblasts into myotubes with parallel orientation, to ultimately form aligned myofibers to compensate for the muscle loss.[4] For skeletal muscle, myotube alignment is difficult to achieve on flat surfaces, like tissue culture polystyrene (TCPS) which gives randomly organized myotubes.[5] The alignment and differentiation of myoblasts were controlled by microstructure topography[6-7] and ECM proteins-based micropatterned surfaces *in vitro*.[8] Since the early use of collagen (COL) to functionalize biomaterial surfaces,[3, 9-10] various approaches were developed to align COL with nanometric control[11] to guide fibroblasts,[12] and/or differentiate myoblasts.[13] For instance, alignment of COL fibers was achieved via lithography,[14] micro-grooved substrates,[15] microfluidics,[16] electrospinning,[17] magnetic fields,[18-19] flow,[20] stretching,[21] and by rubbing.[22-23] However, these techniques possess certain limitations such as the requirement for specialized instrumentations[24] or microfluidic equipment,[16] mechanical assemblies, and strong electric or magnetic fields, which could damage the COL structure.[17, 19] Aside, the use of the nanostructured surface for cell culture are implemented with soluble factors, such as insulin,[1, 25] dexamethasone,[26-27] and insulin-like growth factor (IGF-1),[28] to trigger, support or even accelerate the regeneration

or differentiation processes. Polyphenols consumption is known to contribute to muscle health due to their antioxidant and anti-inflammatory properties. It was shown *in vitro* that polyphenol-rich plum extract treatment enhanced the size of C2C12 mouse myoblasts and accelerated their differentiation.[29] Previously, we reported the use of tannic acid (TA) to develop hydrogen-bonded layer-by-layer (LbL) nanocoatings of COL type I using the dipping method.[30-31] Hydrogen-bonded TA LbL with neutral polymers offer tunable stability over wide pH range, thanks to the pKa of TA.[32] In 2018, Park *et al.* introduced the brushing method, using a paintbrush, to functionalize a surface with chitosan/alginate LbL films for drug delivery, however no alignment of macromolecules was investigated.[33] The brushing process was then used to align a monolayer of clay nanotubes allowing the orientation of human fibroblasts and mesenchymal stem cells along the axis of nanotubes.[34] Mimicking natural plywood, the brushing method was used to develop hierarchically structured hydroxyapatite micro- to nano-fibers/alginate films.[35]

Herein, we report a potent and simple brushing LbL method to develop oriented COL type I based nanocoating*, i.e.,* TA/COL LbL film (Figure 1). Unlike dip-coating, this method is fast, requiring only a few seconds of deposition time for one layer. Moreover, it does not require specific or expensive instrumentation. Built at acidic pH, the oriented TA/COL LbL nanofilms released TA in solution upon contact with a physiological medium with a minor loss of thickness. After characterization of COL fibers orientation, human myoblasts (C25CL48) were seeded in a differentiation medium on the oriented TA/COL film, ended by COL. The alignment and differentiation of the cells were studied after 12 days of culture in comparison to nonoriented TA/COL films, obtained by the dipping method, uncoated glass, and TCPS (polystyrene) substrates.

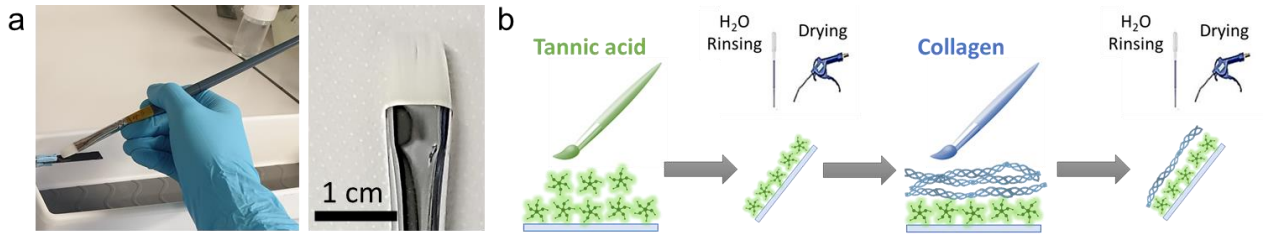

Figure 1. (a) Manual brushing experimental set-up using nylon paintbrush, (b) Schematic representation of the brushed LbL films buildup. Paintbrush image from stockio.com for commercial use.

Results and discussion

The brushing method aligns collagen fibrils in TA/COL LbL films. The buildup of brushed TA/COL films was performed manually on silicon or glass substrate using a nylon paintbrush at each deposition of TA and COL, alternating with a rinsing step and a drying step (Figure 1 and Supplementary video 1). Based on previous work on dipped TA/COL LbL films, an anchoring layer of a poly (ethylene imine) was deposited to allow a homogeneous distribution of COL on the substrate.[31] The brushed film buildup was optimized using different concentrations of TA, two types of paintbrush (Figure S1 in the SI), two angles of the paintbrush to the substrate and two different rinsing solutions (Figure S2-6 in the SI). The rinsing and drying procedures were chosen to sustain COL orientation and according to Park et al,[33] *i.e.* by pipetting and drying in a vertical direction along the brushing direction. Nonoriented TA/COL LbL films were obtained using the conventional dipping method. Figure 2a shows the buildup of brushed and dipped TA/COL films. After 8 deposited bilayers, the thickness of the brushed TA/COL film was around 50 ± 1.5 nm in comparison to 167 ± 19 nm for the dipped film. The buildup by the brushing method follows strictly a linear growth ($R^2 = 0.999$) with COL and TA thickness increments of 4.6 ± 1 and 1.3 ± 0.7 nm, respectively. The greater thickness increment of COL is probably due to its higher

molecular weight (300 000 g/mol) compared to TA with only 1 702 g/mol. Indeed, isolated COL deposited on mica substrate has a thickness of around 2.8 ± 0.2 nm. In citrate buffer, COL tends to form large bundles of around 5.7 nm in thickness which can justify the higher thickness of COL adlayers (Figure S7 in the SI). The size of the TA molecule was determined at 1.3 ± 0.5 nm by dynamic light scattering (Figure S8 in the SI).

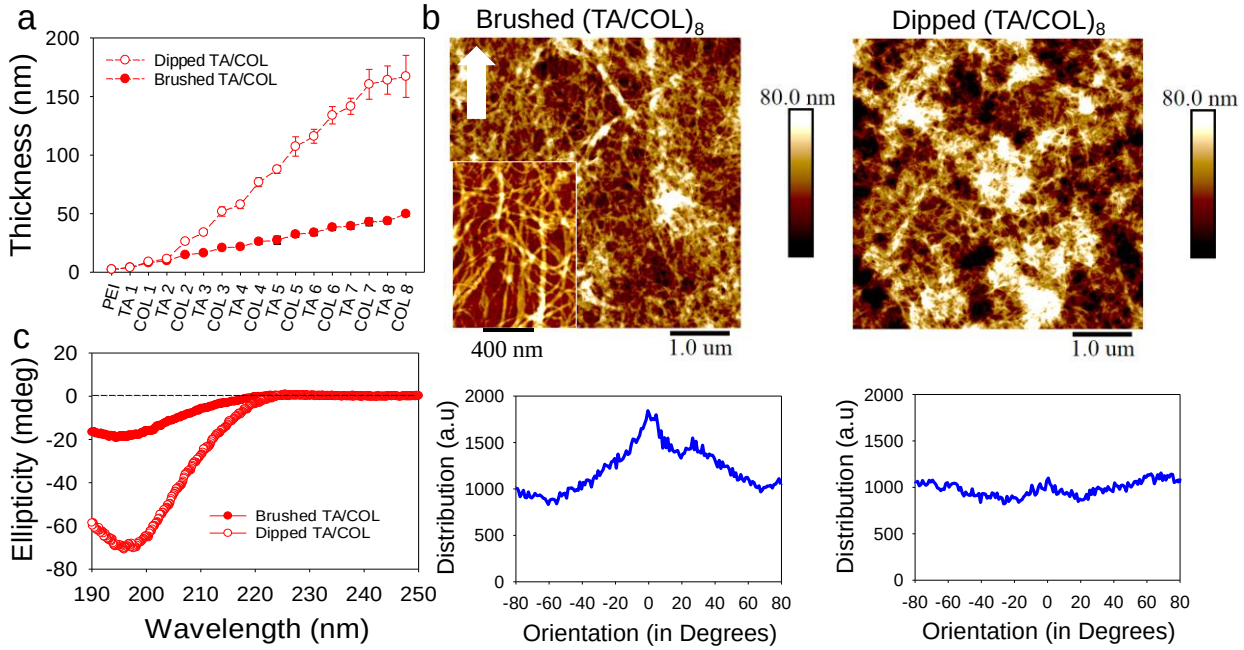

Figure 2. Physico-chemical characterization of the brushed and the dipped TA/COL films. (a) Evolution of the thickness, followed by ellipsometry in dry state, as a function of the last deposited layer (mean and standard deviation from three different samples). The standard deviation of the brushed films is not visible due to the scale of the y-axis (the values are gathered in Table S1 in the SI, Figure S5b in the SI). (b) Typical AFM topography images of the $(TA/COL)_8$ films and the orientation distribution graphs calculated by Image J and as an inset the zoom of the topography. The brushing direction, visible on the video camera, is indicated by the white arrow. (c) Circular dichroism spectra of the TA/COL films.

The surface topography of both TA/COL films was characterized by Atomic Force Microscopy (AFM) in dry state by scanning random areas of various sizes, from 5×5 to 1×1 µm², on the sample

surface. Fibrillary structures were observed for the brushed and dipped TA/COL films (Figure 2b). In the case of the brushed TA/COL film, the alignment of COL fibers was visible (zoom-in Figure 2b) and quantified on the AFM topography image using "OrientationJ" (Figure S4 in the SI). The diameter of the COL fibers was 60 ± 8 nm. The orientation distribution graph of the brushed TA/COL films shows a broad peak at 0° indicating that some COL fibers are oriented between -45° and +45° (Figure 2b) unlike the dipped TA/COL films showing randomly distributed COL fibers with a flat distribution graph. Figure S9 in the SI shows different AFM images from four different brushed TA/COL films at different scales, with even sharper peak at 0° (the brushing direction) in the orientation distribution graph at higher magnification. The degree of COL orientation of the brushed TA/COL films decreases by increasing the number of layer pairs with a complete loss at 16 bilayers (Figure S10 in the SI). This might be due to the loss of effective shear of the brushing by increasing the thickness of underlying LbL film. The secondary structure of COL was then determined by circular dichroism (CD). In solution, COL usually displays characteristic optical activity in the far UV spectrum with a small positive peak around 220-225 nm and a large negative peak in the range 197-200 nm. The CD spectrum of both the brushed and dipped TA/COL films shows a broad negative peak around 197 nm (Figure 2c). The intensity of the negative peak of brushed TA/COL films is lower than the dipped film, which could be explained by the difference in thickness of both films. No significant positive peak at 225 nm was observed in both cases. Generally, the absence of the positive peak at 225 nm, associated with the triple helix, is an indication of partial to full denaturation of COL.[36] However, COL hydrogels crosslinked by TA were reported to sustain COL native conformation with no positive peak (225 nm).[37] The absence of the positive peak of COL solutions was also observed at around 30°C, at which the triple helix structures assemble through fibrillogenesis into highly organized fibrils.[38] In

the following, the brushed and dipped $(TA/COL)_8$ films will be named the oriented and the nonoriented TA/COL films, respectively.

The tannic acid in solution triggers myoblasts' elongation. Before seeding human myoblasts on TA/COL films to study their differentiation and orientation, we first analyzed the cytotoxicity of TA in solution. Figure S11 in the SI shows that TA is toxic to human myoblasts with less than 70% of viability after 24 h of contact at concentrations above 33 µg/mL. For instance, the cell viability was close to zero (0.3±0.1 %) above 375 µg/mL of TA. The treatment of myoblasts with TA shows an important change in the cell area and morphology for concentrations below 33 µg/mL (Figure 3).

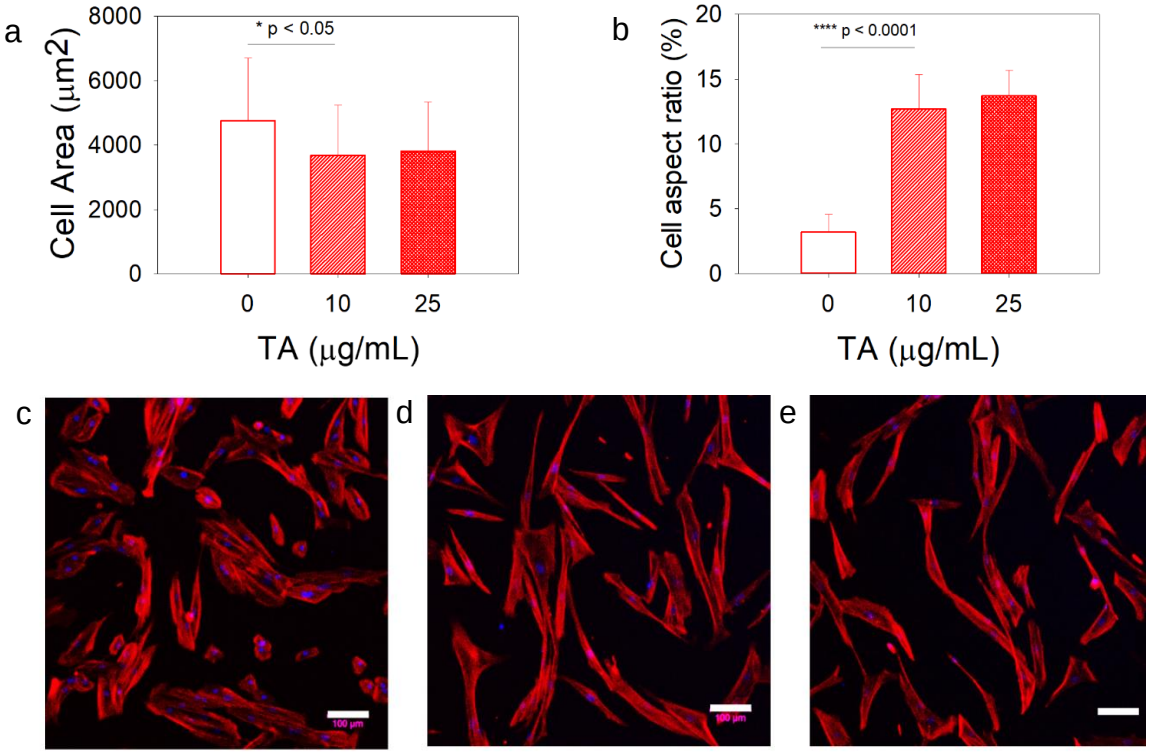

Figure 3. Effect of TA in solution on human myoblasts (C25 CL48) morphology after 24 h of culture. (a) Cell area calculated and (b) cell aspect ratio of the myoblasts, (c-d) Confocal images of the cells in contact with (c) 0, (d) 10, and (e) 25 µg/mL of TA solutions (Scale bars = 100 µm) after F-actin labeling (red, phalloidin) and nuclei labeling (blue, Hoechst 33342).

Such an effect was quantitatively evaluated in terms of cell area (Figure 3a) and aspect ratio (Figure 3b), using ImageJ. The incubation with TA induced the elongation of cells resulting in roughly 20% reduced cell area and 4 times higher aspect ratio compared to the cells without TA treatment. In the absence of TA, cells were well spread with no significant elongation (Figure 3c). At 10 and 25 μg/mL after 24 h of incubation, myoblasts showed elongated morphology, also known as a pro-differentiation phenotype, which is an essential precursor for cell fusion (Figure 3d and Figure 3e).[39] Until now, no studies on the effect of TA on the differentiation of myoblasts was performed, only the uptake of TA by myoblasts was reported so far.[40] The observed elongation in the presence of TA is consistent with the studies related to the effect of polyphenols on muscle pathology and myotubule formation.[29, 41]

Human myoblasts align and differentiate on the oriented TA/COL films. The orientation and differentiation of human myoblasts were investigated on TA/COL LbL films via immunocytochemistry to stain heavy chain myosin (MHC) sarcomere protein, typically expressed by mature myotubes. Myoblasts were seeded on LbL samples and uncoated glass for 24 h in complete growth medium followed by 12 days in differentiation medium, without any other supplements. We checked that the nanostructure of the oriented TA/COL film was preserved after 3 days of incubation in the DMEM medium (Figure S12 in the SI). Confocal microscopy images were recorded on day 12 and treated by OrientationJ, as shown in Figure 4. On the oriented TA/COL nanofilms, the immunostaining showed that the cells aligned and differentiated into multinucleated long myotubes with the oriented arrangement of myonuclei (Figure 4a). Myofibers' actin filaments appeared aligned which was expressed as a broad peak at 0°, i.e., the brushing direction (Figure 4b).

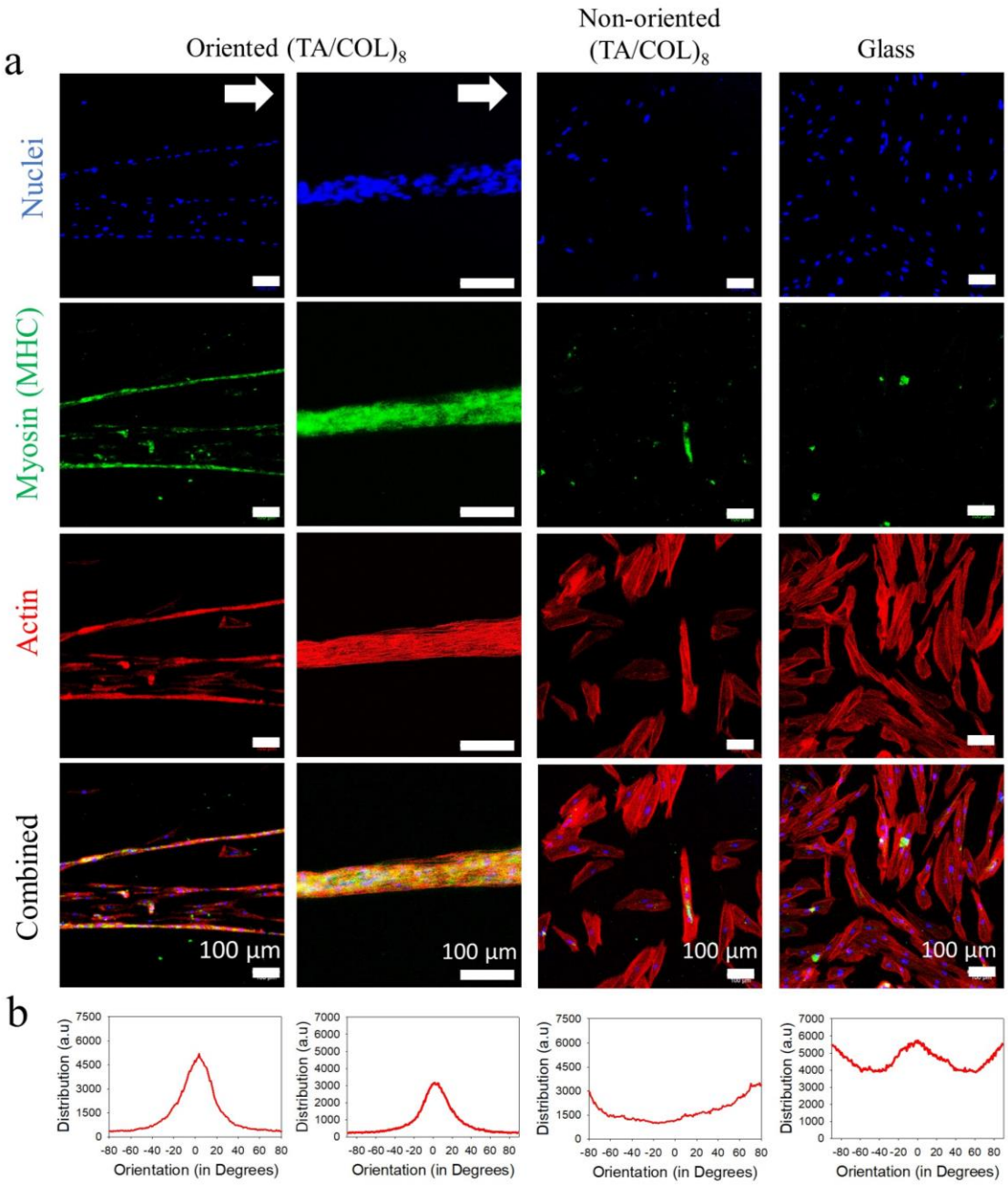

Figure 4. Orientation and differentiation of human myoblasts after 12 days of culture on the oriented and the nonoriented TA/COL films, and uncoated glass. (a) Confocal microscopy images at different channels with nuclei (in blue), myosin heavy chain (in green), and actin filament (in red). The white arrow represents the brushing direction (Scale bar = 100 µm). (b) The orientation distributions were calculated from the actin cytoskeleton via ImageJ. All the confocal microscopy images are representative of three experiments (three samples each).

Such myotubes formed thicker myofibers of diameter around 100 µm, i.e., approximately equivalent to the diameter of human muscle fibers (Figure 4a and Figure S13 in the SI). At this stage, some myofibers were also observed to neglect the LbL orientation (data not shown). On the nonoriented TA/COL nanofilms, randomly distributed and elongated myoblasts can be observed as in the case of the glass control substrate with almost no myosin staining (Figure 4a). In comparison, randomly distributed myoblasts and shorter myotubes (fewer fused nuclei) were observed on TCPS (Figure S14 in the SI). Regarding the cell morphology, a strong difference can be observed after 12 days of culture (Figure S15 in the SI). Of critical importance in muscle regeneration, the differentiation of myoblasts follows a contact-dependent mechanism, where movement or migration to come closer, fuse, and form myotubes is important.[1, 3] The myoblasts movement was recorded by time-lapse video for the first 48 h in contact with the oriented TA/COL films in the growth medium (Supplementary video 2). The oriented COL LbL guides undifferentiated myoblasts to align in the direction of the brushing and form denser cell regions favoring later the fusion and differentiation into myotubes in the differentiation medium. On the nonoriented TA/COL films and the uncoated glass surface, a random movement of cells was observed on 48 h time-lapse video (Supplementary videos 3 and 4, respectively). We then assessed the cell density on the different coatings after 12 days of differentiation. Based on the mean values of total nuclei, the oriented TA/COL film presented the same cell density as the uncoated glass substrate. In the case of nonoriented TA/COL film, the cell density is one-third compared to the glass control (Figure 5a). TA/COL films switch significantly from biocompatible to cytotoxic towards human myoblasts depending on the buildup method. TA/COL LbL films were shown to be stable in the physiological medium with a part of TA released.[30-32] We then monitored the TA release of both TA/COL films. Upon incubation in PBS at room temperature, the release of TA

followed an initial linear kinetic with roughly 86% of release within the first 4 h, which then stabilized over 1-4 days. The nonoriented TA/COL films, *i.e.* $(TA/COL)_8$, released approximately 9 times more TA than the oriented film with 37 ± 3.6 µg/mL vs 4.2 ± 0.5 µg/mL, respectively (Figure 6). The difference in the amount of released TA can be explained by the thickness of the films (Figure 2a).

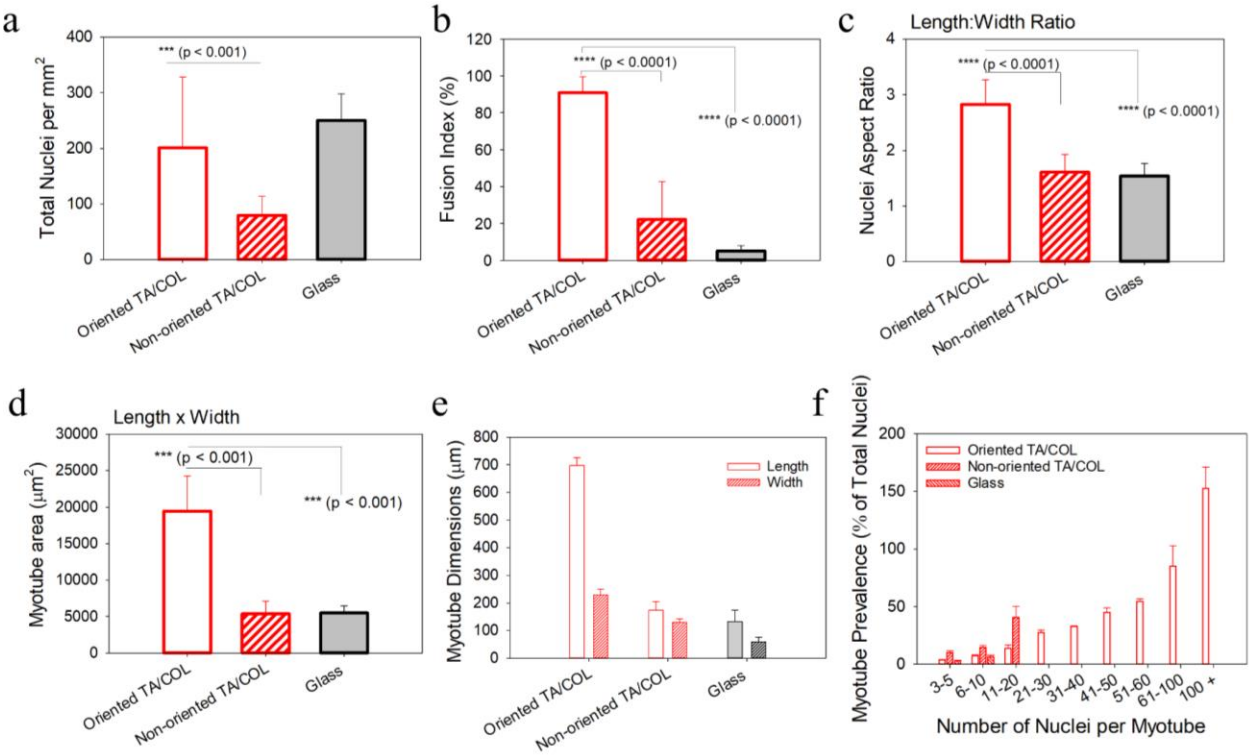

Figure 5. Quantitative information from immunofluorescence images (surface image area 691 456 µm²) of human myoblast differentiation after 12 days of culture on TA/COL LbL films. (a) Cell density (b) fusion index, (c) aspect ratio of nuclei, (d) area of myotubes, and (e) their dimensions, (f) myotube prevalence. Three different fields were measured for each condition and the experiments were conducted in triplicate.

The quantity of TA released by the nonoriented film (37 ± 3.6 µg/mL) is close to the cytotoxicity threshold towards myoblasts leading to a lower cell density in comparison to the glass control.

This effect can even be strengthened by local release of TA at the surface of the nanocoating as found for the antibacterial effect on the same system.[31]

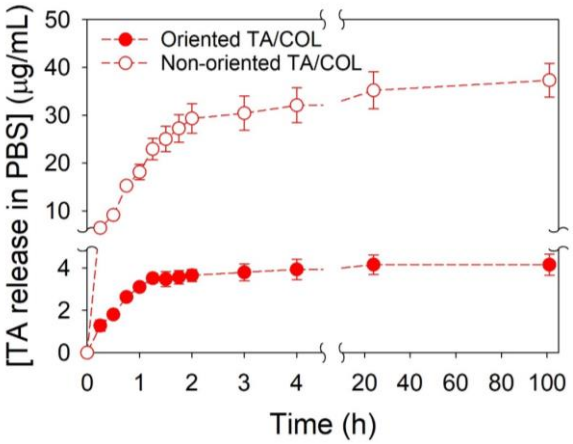

Figure 6: Cumulative release profiles of TA from the oriented and the nonoriented TA/COL films in contact with PBS pH 7.4 at room temperature.

Lastly, we evaluated the final myotube formation after 12 days of differentiation by the quantification of the fusion index (defined as a ratio of nuclei contained in myotubes, with ≥2 nuclei, to the total nuclei), the aspect ratio of nuclei, the area, dimension and prevalence of myotubes (defined as the number of nuclei per myotube represented as % of total nuclei)[42] (Figure 5b-f). The oriented TA/COL films showed an ability for the development of aligned myotubes from human myoblasts. Indeed, the fusion index calculated on the oriented TA/COL films is around 90 ± 9 % in comparison to 22 ± 14 % for the nonoriented films and 5% for glass control (Figure 5b). This indicates that approximately all the attached and proliferated myoblasts differentiated into myotubes after 12 days of culture on the oriented TA/COL films. Interestingly, the nanotopography of TA/COL films not only impacted the myoblast differentiation, but also the morphology of the nuclei (Figure S16 in the SI). Elongated nuclei with an aspect ratio of around 2.8 were observed on the oriented TA/COL films, whereas a broad shape morphology with the aspect ratio of approximately 1.5-1.6 is observed on the nonoriented TA/COL film and the glass

control (Figure 5c). Myoblasts were reported to exhibit deformed nuclei morphologies depending on surface nanostructures.[39] Besides the fusion index, we observed significant differences in the area and dimensions of myotubes formed on the different samples. Myotube area on the oriented TA/COL films is around 3.6 times higher than the one on the nonoriented film, the glass control (Figure 5d). Consistent with the myotube area, the myotubes on the oriented TA/COL films are 698 ± 28 μm in length and 230 ± 21 μm in width *i.e.,* approximately 4 times longer and 2 times thicker than the ones on the nonoriented films and glass (Figure 5e). We can notice the presence of myotubes with more than 30 to 100 nuclei only on the oriented TA/COL films (Figure 5f). To investigate the impact of TA release on the myoblasts' differentiation, TA was washed out from the oriented TA/COL films, by 24 h incubation in PBS medium, prior to the cell seeding. After 12 days of culture, myoblasts appeared partially elongated. Actin cytoskeleton of cells were randomly oriented as shown by Image J treatment (Figure S17 in the SI) with the maxima of the orientation distribution not centered at 0° (the brushing direction). In contrast to the oriented TA/COL films (not washed by PBS), a significantly lower number of cells showed myosin labeling and the obtained myotubes were not aligned along the oriented COL fibers of PBS-incubated films (Figure S17 in the SI). In addition to COL-induced orientation of myoblasts, TA release appears to trigger efficient cell differentiation, as shown in Figure 4. Indeed, on PBS-incubated oriented TA/COL films, the fusion index of myoblasts was of 69 ± 22 % vs 91 ± 9 % on the untreated films with a similar nuclei aspect ratio, myotube area, dimensions, and prevalence (Figure S18 in the SI). The comparison with TCPS as control substrate is also shown in Figure S18 in the SI, presenting comparable results as the glass substrate. To confirm the synergistic role of TA release and COL orientation, we performed experiments on nonoriented TA/COL films having similar thickness (54 ± 4 nm) and amount of TA released (5.9 ± 1.2 μg/mL) as the oriented TA/COL films, i.e. dipped

$(TA/COL)_3$ films (Figure S19 in the SI). After 12 days of incubation on the nonoriented $(TA/COL)_3$ film in the differentiation medium, elongated and randomly distributed myoblasts were observed with no myosin expression (no green staining), similar to the nonoriented film $(TA/COL)_8$ (Figure S20a in the revised SI) with a higher cell density due to the lower amount of TA released in the supernatant (Figure S20c in the SI). The glass control was also performed for comparison (Figure S20b in the SI). On the nonoriented $(TA/COL)_3$ and $(TA/COL)_8$ films, the fusion index was similar at 17 ± 7% and 22 ± 14%, respectively, and the aspect ratio of the nuclei was approximately 1.5 (Figure S20d-e in revised SI). The dimensions of the myotubes were different, with cells being more elongated in the nonoriented $(TA/COL)_3$ than $(TA/COL)_8$ film with a length/width of 185 ± 61 µm/24 ± 8 µm vs 173 ± 31 µm/129 ± 13 µm, respectively (Figure S20f-h in the SI). Regarding the prevalence of myotubes, no myotubes with more than 10 nuclei were observed on the nonoriented films $(TA/COL)_3$. In summary, the absence of COL orientation prevents the orientation of myoblasts as well as their differentiation into myofibers and the lower amount of TA released allows for better cytocompatibility, the presence of more elongated myotubes but with fewer nuclei on the nonoriented films. The orientation of the myoblasts is due to the orientation of the COL chains and their elongation to the TA released into the supernatant by the oriented film which leads to their differentiation into myofibers. Myofibers of length around 1.7 mm reconstructed from confocal images were observed on the oriented TA/COL films, showing the distribution of the nuclei (blue), myosin heavy chain (in green) and actin filament (in red). The myotube dimensions obtained might range from hundreds of micrometers to millimeters, depending on the size of the sample.

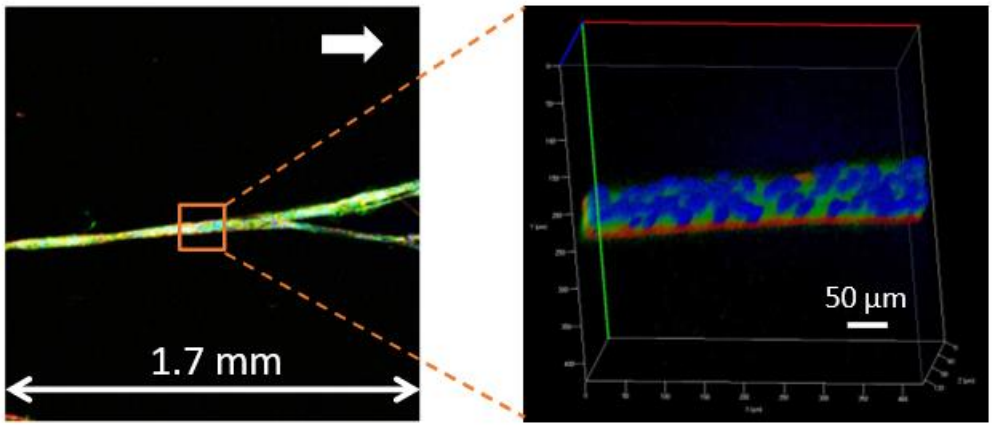

Figure 7. Confocal microscopy images of a human myotube, obtained from myoblasts after 12 days of culture on the oriented TA/COL film, with combined channels of nuclei (in blue), myosin heavy chain (in green) and actin filament (in red). Zoom in 3D reconstructed confocal image is shown on the right.

Conclusion

We demonstrated that the brushed LbL films appear to be a potent and simple way to produce surfaces with aligned topography using macromolecules of high aspect ratio, such as COL. In comparison to the other methods developed so far, there is no need for sophisticated apparatus. The aligned TA/COL nanofilms influenced the cells behavior, by improving their adhesion to a substrate, influencing their morphology, alignment, and differentiation. The differentiation of human myoblasts was obtained in 12 days when seeded on the oriented TA/COL films in differentiation medium without any other supplement thanks to two distinct properties: (i) COL orientation which helps to align myoblasts favoring their close contact, and (ii) TA release which favors the differentiation. On the TA/COL films, the topography cues and the strong links between cells and the collagen can be further used to mimic the complexity of *in vivo* conditions and design

model tissues to regenerate anisotropic tissues, the treatment of injuries or diseases or for pharmacology research.

Experimental Section

Materials. Collagen (COL, purified type I from calf, Symatese, France), tannic acid (TA, Mw = 1701.2 g/mol, Sigma-Aldrich, France), poly(ethylene imine) (PEI, branched, 30% w/w aq. solution, Mw = 50 000–100 000 g/mol, Alfa Aesar, Germany), citric acid monohydrate (Mw = 210.14 g/mol, Sigma-Aldrich), sodium citrate tribasic dihydrate (Mw = 294.10 g/mol, Sigma-Aldrich), Dulbecco's phosphate buffer saline (PBS, L0615, Dominique Dutscher, France), Dulbecco's Modified Eagle Medium (DMEM, L0103, Dominique Dutscher, France), sodium dodecyl sulfate (Prolabo, Poland), NaCl (VWR), HCl, and NaOH (Sigma-Aldrich) were used as received.

Collagen and tannic acid solutions. All solutions were prepared freshly prior to use except COL. Deionized water (Milli-Q, 18.2 MΩ·cm at 25 °C) supplied by Advantage A10 (MERCK) was used in the entire study. The pH values were adjusted by using 0.1 M HCl or 0.1 M NaOH solution prepared in deionized water. Prior to thin film buildup, all the solutions were filtered using a 0.20 μm filter (Sarstedt, no. 831826001) to remove any impurity or undissolved substances. The citrate buffer used in this study was prepared at pH 4 by mixing 41 mL of 0.1 M sodium citrate tribasic dihydrate solution and 59 mL of 0.1M citric acid monohydrate solution. PEI solution was prepared at 0.1 mg/mL in 0.15 M sodium chloride (NaCl) aqueous solution (no pH adjustment). TA solution was prepared at 0.5 mg/mL in citrate buffer at pH 4 (otherwise stated) and kept in dark to avoid its photooxidation. COL solution was prepared at 1 mg/mL in citrate buffer at pH 4 (otherwise stated) by overnight agitation using a magnetic stirrer at 4 °C.

TA/COL LbL buildup. Silicon wafers or microscopic glass slides were cut using a sharp diamond pen to obtain 1 × 6 cm² rectangular substrates. Silicon wafers were cleaned with ethanol/water (50% v/v) solution for 15 min prior to their use. Glass substrates were cleaned by immersing in the solutions of 10 mM SDS and 0.1 M HCl at 70°C for 10 min each, followed by extensive rinsing with deionized water. Prior to the film buildup, the substrates were plasma etched for 2.5 min with air using Harrick PDC-002-HP at high RF level to remove particles and to render the surface negatively charged and hydrophilic. PEI, a branched polycation, was used as precursor layer on each substrate before LbL buildup. Immediately after plasma cleaning, the substrate was dipped in PEI solution for 10 s, rinsed twice with ultrapure water for 5 s and dried with filtered compressed air. The substrate is then a positively charged surface ensuring a good anchoring of the films. Oriented TA/COL based films were obtained by the brushing method. The PEI-functionalized substrate was clipped with a support in a horizontal direction facing upwards to brush the solutions always in the same direction with nylon paintbrush with hard bristles (Søstrene Grenes, Aarhus, Danemark). Horsehair paintbrush with soft bristles (Søstrene Grenes, Aarhus, Danemark) was also used at the optimization of the buildup. Regarding the optimized buildup of oriented TA/COL films, TA and COL solutions were brushed manually with the nylon paintbrush tilted at an angle of 30° to the substrate and left to dry for 10 s, followed by two rinsing steps with ultrapure water using a disposable pipette and dried with filtered compressed air at 2.5 bar, both in a vertical direction along the brushing direction. With n the number of bilayer deposition, the following brushed PEI-$(TA/COL)_n$ films were studied and named oriented TA/COL film with $n = 8$. Nonoriented TA/COL films were obtained by the dipping method. The PEI-functionalized substrate was immersed in TA solution for 10 s, followed by two rinsing steps by dipping in ultrapure water for 5 s and dried by filtered compressed air. The same process was followed to

deposit COL adlayer, to obtain one bilayer. The process was repeated n times to obtain brushed PEI-$(TA/COL)_n$ named nonoriented TA/COL film with n = 8. Once the desired film architecture is achieved, the homogeneous part of the sample (in the center of the substrate) was selected and cut to obtain 1×1 cm2 area samples to characterize the film properties.

Ellipsometry. The film thickness was measured, after rinsing with water and drying by compressed air, using an Ellipsometer (SD2300, PLASMOS) with an incident laser beam (632.8nm) and a constant angle of 45°. Refractive index was assumed to be constant and equal to 1.465 for all the measurements. The dry thickness values reported here are the average values with standard deviation of three individual LbL buildup experiments. Ten measurements were performed at random areas on each one of the multilayer sample surfaces. The routine ellipsometry measurements might show insignificant differences in absolute dry thickness and a more advanced ellipsometry equipment would be required for accurate measurements. However, the thickness readings are satisfactorily accurate to compare the buildup of different LbL films reported here.

Atomic Force Microscopy (AFM). COL/TA films, in dry state using nitride coated silicon tips on a nitride cantilever (Model ScanAsyst-Air, with force constant k = 0.4 N/m and frequency fn =70 kHz) and Peak Force Tapping (ScanAsyst) mode. The images were obtained at a scan rate of 1 Hz with a resolution of 512 × 512 pixels. The data analysis was performed using NanoScope Analysis software version 1.7. Random areas of the samples were scanned to obtain typical topography images. Open-source software Image J was used to determine the orientation of COL fibres using plugin "Orientation J" developed at the École Polytechnique Fédérale de Lausanne (EPFL).[43] Firstly, AFM images were converted into grey scale (8-bit) and then the program computes the local orientation properties. From this software, a visual directional analysis is obtained in which the orientation is encoded in color following the color-coding reference image.

An orientation histogram can be calculated by taking into consideration few parameters such as a Gaussian window of 1 pixel to account for the smallest possible nanostructure, and a minimum coherency and energy of 1% to eliminate the effect of isotropic areas. The distribution of orientation for TA/COL multilayers was adjusted to 0°. The same method was applied on fluorescence microscopy images to determine the orientation of cells seeded the different substrates.

TA release in physiological conditions. TA release from the oriented and the nonoriented TA/COL films in contact with PBS buffer at room temperature was followed by measuring the absorbance intensity at 277 nm using a spectrofluorometer (SAFAS Xenius XC). COL used in the study showed no absorption at this wavelength. First, a calibration curve of TA was obtained by measuring the absorbance intensity at 277 nm for different concentrations of TA in PBS buffer. The samples were prepared on glass slides with final dimensions of 1×1 cm^2. Five hundred microliters of PBS buffer at pH 7.4 at room temperature was put in contact with the films. One hundred microliters of the supernatant were withdrawn and put in a UV-Star 96-well plate (Greiner bio-one) to measure the absorbance at 277 nm. To compensate 100 µL of supernatant loss, 100 µL of fresh PBS was added.

Human Myoblasts (C25CL48) culture. The initial biopsies from which the human myoblasts cell lines were isolated were provided by MyoBank, the tissue bank from The Institut de Myologie in Paris, affiliated to EuroBioBank. MyoBank has receive the approval from the French Ministry of Higher Education, research, and Innovation to distribute human samples for research (Authorization AC-2019-3502). Cells were maintained in TCPS flasks in a humidified 5% CO2 incubator at 37°C. The experiments were conducted from cell passage 5-9. The cells were cultured in Dulbecco's Modified Eagle Medium (DMEM) + 4.5 g/L glucose supplemented with 20% fetal

bovine serum, and 1% penicillin and streptomycin, named as “growth medium (GM)”. The cells were pre-cultured to reach around 70% confluence.

Human myoblasts’ viability. The cell (3000/well) were seeded in a TCPS 96-well plate and allowed to proliferate for 24 h. The cells were rinsed with PBS, and 100 µL of TA solutions at different concentrations prepared in the growth medium was dispensed in the wells. After 24 h of contact with the TA, followed by a PBS rinsing step, 100 µL of the CellTiter-Glo 2.0 assay reagent (Promega, G9242) was added and incubated in a shaker for 15 min at room temperature. Finally, luminescence was recorded using a spectrofluorometer (SAFAS Xenius XC). The cell area was calculated using Freehand tool in the ImageJ software and presented as a mean value of 40 cells on five individual images (200 cells in total).

Myoblasts differentiation. The freshly prepared TA/COL film samples were UV sterilized in dry state for 20 min before the cell seeding. 20,000 cells/mL were seeded on each tested sample and allowed to proliferate for 24 h. Then, the growth medium was switched to differentiation medium (DM) (DMEM high glucose supplemented with 2% horse serum and 1% penicillin and streptomycin). Cell differentiation was followed for 12 days. DM was replaced with fresh DM after every 3-4 days. After 12 days of differentiation, cells were fixed with 500 µL of 4% PFA for 15 min at room temperature, followed by two rinsing steps using 1mL PBS, 5 min each. The cells were permeabilized by incubating in 1 ml of 0.5% Triton X-100 in PBS for 4 min, followed by three rinsing steps using 1mL PBS, 5 min each. The cells were incubated in 1% BSA solution in PBS for 1h at room temperature to block unnecessary sites to minimize background noise. To stain heavy chain myosin, 500 µL of the primary antibody (MF-20, AB_2147781, 0.039 µg/mL, 1/564 dilution in 0.1% BSA in PBS) was added for 2h at room temperature, in dark. After rinsing with PBS, cells were incubated in 500 µL of Abcam 150113 Goat Anti-Mouse IgG H&L (Alexa Fluor®

488) 1/500 diluted in 0.1 % BSA in PBS for 1 h at room temperature, in dark followed by two rinsing steps with PBS (2 x 1000 µL). Then, the cells were incubated in 500 µL of phalloidin-TRITC solution (dilution 1/800) in PBS for 30 min at room temperature, in dark followed by PBS (1000 µL) rinsing step. Finally, 500 µL of Hoechst 33342 (Invitrogen, B2261, dilution 1/1000) at 5 µg/ml in PBS were added at room temperature for 10 min to stain nuclei. Finally, the samples were mounted in transparent glass slides to observe under Zeiss LSM 710 confocal microscopy. For cell viability in contact with different concentrations of TA solutions, only actin filament (phalloidin-rhodamine) and nuclei (Hoechst 33342) were stained following a similar protocol as above. The quantitative information calculated from immunofluorescence images of human myoblast differentiation after 12 days of culture on the oriented and the nonoriented TA/COL films, uncoated glass and TCPS were calculated on a given surface image of area 691 456 μm^2. Three different images were measured for each condition and the experiments were conducted in triplicate.

Statistical analysis. The two-tail student t-test was performed on all cell biology experimental data to determine the statistical significance of differences between the oriented and the nonoriented multilayer films with uncoated glass substrates (control). The obtained p-values are indicated on the corresponding graphs with symbols such as *, **, ***, and **** for $p \leq 0.05$, 0.01, 0.001, and 0.0001, respectively.

ASSOCIATED CONTENT

Supporting Information. Optimization of TA/COL brushing method, AFM topography/cross-section of isolated COL fibers on mica, hydrodynamic size of TA, “OrientationJ” color coded analysis of the AFM topography images of brushed and dipped TA/COL films, AFM topography

and OrientationJ analysis of oriented $(TA/COL)_4$, $(TA/COL)_8$, and $(TA/COL)_{16}$, *in vitro* cytotoxicity of TA on human myoblasts, AFM topography/orientation of oriented TA/COL after 3 days incubation in DMEM medium, myoblasts after 12 days of differentiation on oriented TA/COL and TCPS, morphology of myoblasts after 12 days of differentiation, TA release from the TA/COL films, morphology of isolated nuclei on differentiation day 12, differentiation/orientation of myoblasts oriented TA/COL_PBS films, quantitative information for oriented TA/COL_PBS films and controls on differentiation day 12, Physico-chemical characterization of the nonoriented $(TA/COL)_3$ and myoblasts after 12 days of differentiation the nonoriented $(TA/COL)_3$. The video 1, video 2, video 3 and video 4 are available as separate files (.avi). Supporting Information is available free of charge.

AUTHOR INFORMATION

Corresponding Author

*** Dr. Fouzia Boulmedais -** Université de Strasbourg, CNRS, Institut Charles Sadron, UPR 22, Strasbourg Cedex 2, 67034, France

Email: fouzia.boulmedais@ics-cnrs.unistra.fr

Author Contributions

The manuscript was written through contributions of all authors. All authors have given approval to the final version of the manuscript.

Funding Sources

Institut Carnot MICA DIAART project, Fonds Régional de Coopération pour la Recherche of Région Grand Est ERMES project and International Centre for Frontier Research in Chemistry (icFRC) are acknowledged for financial support.

ACKNOWLEDGMENT

Sarah Benmalek-Kehili and Christine Affolter-Zbaraszczuk are acknowledged for their technical help. M.H.I. thanks the Higher Education Commission (HEC) Pakistan for his Ph.D. scholarship. Institut Carnot MICA DIAART project, Fonds Régional de Coopération pour la Recherche of Région Grand Est ERMES project and International Centre for Frontier Research in Chemistry (icFRC) are acknowledged for financial support.

REFERENCES

1. Beldjilali-Labro, M.; Garcia Garcia, A.; Farhat, F.; Bedoui, F.; Grosset, J.-F.; Dufresne, M.; Legallais, C., Biomaterials in Tendon and Skeletal Muscle Tissue Engineering: Current Trends and Challenges. *Materials* **2018,** *11*, 1116.
2. Järvinen, M. J.; Lehto, M. U. K., The Effects of Early Mobilisation and Immobilisation on the Healing Process Following Muscle Injuries. *Sports Med.* **1993,** *15*, 78-89.
3. Vandenburgh, H. H.; Karlisch, P.; Farr, L., Maintenance of highly contractile tissue-cultured avian skeletal myotubes in collagen gel. *In Vitro Cell. Dev. Biol.* **1988,** *24*, 166-174.
4. Meyer, G. A.; Lieber, R. L., Elucidation of extracellular matrix mechanics from muscle fibers and fiber bundles. *J. Biomech.* **2011,** *44*, 771-773.
5. Stern-Straeter, J.; Riedel, F.; Bran, G.; Hörmann, K.; Goessler, U. R., Advances in skeletal muscle tissue engineering. *In Vivo* **2007,** *21*, 435-444.
6. Lam, M. T.; Sim, S.; Zhu, X.; Takayama, S., The effect of continuous wavy micropatterns on silicone substrates on the alignment of skeletal muscle myoblasts and myotubes. *Biomaterials* **2006,** *27*, 4340-4347.
7. Charest, J. L.; García, A. J.; King, W. P., Myoblast alignment and differentiation on cell culture substrates with microscale topography and model chemistries. *Biomaterials* **2007,** *28*, 2202-2210.
8. Bajaj, P.; Reddy, B., Jr.; Millet, L.; Wei, C.; Zorlutuna, P.; Bao, G.; Bashir, R., Patterning the differentiation of C2C12 skeletal myoblasts. *Integr. Biol.* **2011,** *3*, 897-909.
9. Morra, M.; Cassinelli, C.; Cascardo, G.; Cahalan, P.; Cahalan, L.; Fini, M.; Giardino, R., Surface engineering of titanium by collagen immobilization. Surface characterization and in vitro and in vivo studies. *Biomaterials* **2003,** *24*, 4639-4654.
10. Grant, G. G. S.; Koktysh, D. S.; Yun, B.; Matts, R. L.; Kotov, N. A., Layer-By-Layer Assembly of Collagen Thin Films: Controlled Thickness and Biocompatibility. *Biomed. Microdevices* **2001,** *3*, 301-306.

11. Pastorino, L.; Dellacasa, E.; Scaglione, S.; Giulianelli, M.; Sbrana, F.; Vassalli, M.; Ruggiero, C., Oriented collagen nanocoatings for tissue engineering. *Colloids Surf., B* **2014,** *114*, 372-378.
12. Guido, S.; Tranquillo, R. T., A methodology for the systematic and quantitative study of cell contact guidance in oriented collagen gels. Correlation of fibroblast orientation and gel birefringence. *J. Cell Sci.* **1993,** *105 (Pt 2)*, 317-331.
13. Bailey, A. J.; Shellswell, G. B.; Duance, V. C., Identification and change of collagen types in differentiating myoblasts and developing chick muscle. *Nature* **1979,** *278*, 67-69.
14. Xia, Y.; Rogers, J. A.; Paul, K. E.; Whitesides, G. M., Unconventional Methods for Fabricating and Patterning Nanostructures. *Chem. Rev.* **1999,** *99*, 1823-1848.
15. Vernon, R. B.; Gooden, M. D.; Lara, S. L.; Wight, T. N., Microgrooved fibrillar collagen membranes as scaffolds for cell support and alignment. *Biomaterials* **2005,** *26*, 3131-3140.
16. Lee, P.; Lin, R.; Moon, J.; Lee, L. P., Microfluidic alignment of collagen fibers for in vitro cell culture. *Biomed. Microdevices* **2006,** *8*, 35-41.
17. Zhong, S.; Teo, W. E.; Zhu, X.; Beuerman, R. W.; Ramakrishna, S.; Yung, L. Y., An aligned nanofibrous collagen scaffold by electrospinning and its effects on in vitro fibroblast culture. *J. Biomed. Mater. Res. Part A* **2006,** *79*, 456-463.
18. Dubey, N.; Letourneau, P. C.; Tranquillo, R. T., Guided Neurite Elongation and Schwann Cell Invasion into Magnetically Aligned Collagen in Simulated Peripheral Nerve Regeneration. *Exp. Neurol.* **1999,** *158*, 338-350.
19. Guo, C.; Kaufman, L. J., Flow and magnetic field induced collagen alignment. *Biomaterials* **2007,** *28*, 1105-1114.
20. Lanfer, B.; Freudenberg, U.; Zimmermann, R.; Stamov, D.; Körber, V.; Werner, C., Aligned fibrillar collagen matrices obtained by shear flow deposition. *Biomaterials* **2008,** *29*, 3888-3895.
21. Chaubaroux, C.; Perrin-Schmitt, F.; Senger, B.; Vidal, L.; Voegel, J. C.; Schaaf, P.; Haikel, Y.; Boulmedais, F.; Lavalle, P.; Hemmerle, J., Cell Alignment Driven by Mechanically Induced Collagen Fiber Alignment in Collagen/Alginate Coatings. *Tissue Eng., Part C* **2015,** *21*, 881-888.
22. Uto, S.; Miki, M.; Kuwata, Y., Orientation of Cultured Myotube on Rubbed Collagen. *Trans. Jpn. Soc. Med. Biol. Eng.* **2013,** *51,* R-110.
23. Chai, Y.; Okuda, M.; Miyata, M.; Liu, Z.; Tagaya, M., Rubbing-assisted approach for highly-oriented collagen fibril arrays involving calcium phosphate precipitation. *Mater. Chem. Front.* **2021,** *5*, 3936-3948.
24. Vernon, R. B.; Gooden, M. D.; Lara, S. L.; Wight, T. N., Microgrooved fibrillar collagen membranes as scaffolds for cell support and alignment. *Biomaterials* **2005,** *26*, 3131-3140.
25. Ewton, D. Z.; Florini, J. R., Effects of the somatomedins and insulin on myoblast differentiation in vitro. *Dev. Biol.* **1981,** *86*, 31-39.
26. Han, D.-S.; Yang, W.-S.; Kao, T.-W., Dexamethasone Treatment at the Myoblast Stage Enhanced C2C12 Myocyte Differentiation. *Int. J. Med. Sci.* **2017,** *14*, 434-443.
27. Almonacid Suarez, A. M.; Zhou, Q.; van Rijn, P.; Harmsen, M. C., Directional topography gradients drive optimum alignment and differentiation of human myoblasts. *J. Tissue Eng. Regener. Med.* **2019,** *13*, 2234-2245.
28. Fanzani, A.; Colombo, F.; Giuliani, R.; Preti, A.; Marchesini, S., Insulin-like growth factor 1 signaling regulates cytosolic sialidase Neu2 expression during myoblast differentiation and hypertrophy. *FEBS J.* **2006,** *273*, 3709-3721.
29. Alsolmei, F. A.; Li, H.; Pereira, S. L.; Krishnan, P.; Johns, P. W.; Siddiqui, R. A., Polyphenol-Enriched Plum Extract Enhances Myotubule Formation and Anabolism while Attenuating Colon Cancer-induced Cellular Damage in C2C12 Cells. *Nutrients* **2019,** *11*, 1077.

30. Reitzer, F.; Berber, E.; Halgand, J.; Ball, V.; Meyer, F., Use of Gelatin as Tannic Acid Carrier for Its Sustained Local Delivery. *Pharm. Front.* **2020,** *2*, e200002.
31. Iqbal, M. H.; Schroder, A.; Kerdjoudj, H.; Njel, C.; Senger, B.; Ball, V.; Meyer, F.; Boulmedais, F., Effect of the Buffer on the Buildup and Stability of Tannic Acid/Collagen Multilayer Films Applied as Antibacterial Coatings. *ACS Appl. Mater. Interfaces* **2020,** *12*, 22601-22612.
32. Erel-Unal, I.; Sukhishvili, S. A., Hydrogen-Bonded Multilayers of a Neutral Polymer and a Polyphenol. *Macromolecules* **2008,** *41*, 3962-3970.
33. Park, K.; Choi, D.; Hong, J., Nanostructured Polymer Thin Films Fabricated with Brush-based Layer-by-Layer Self-assembly for Site-selective Construction and Drug release. *Sci. Rep.* **2018,** *8*, 3365.
34. Zhao, X.; Zhou, C.; Lvov, Y.; Liu, M., Clay Nanotubes Aligned with Shear Forces for Mesenchymal Stem Cell Patterning. *Small* **2019,** *15*, 1900357.
35. Chen, S.-M.; Gao, H.-L.; Zhu, Y.-B.; Yao, H.-B.; Mao, L.-B.; Song, Q.-Y.; Xia, J.; Pan, Z.; He, Z.; Wu, H.-A.; Yu, S.-H., Biomimetic twisted plywood structural materials. *Natl. Sci. Rev.* **2018,** *5*, 703-714.
36. Velmurugan, P.; Singam, E. R.; Jonnalagadda, R. R.; Subramanian, V., Investigation on interaction of tannic acid with type I collagen and its effect on thermal, enzymatic, and conformational stability for tissue engineering applications. *Biopolymers* **2014,** *101*, 471-483.
37. Brazdaru, L.; Micutz, M.; Staicu, T.; Albu, M.; Sulea, D.; Leca, M., Structural and rheological properties of collagen hydrogels containing tannic acid and chlorhexidine digluconate intended for topical applications. *C. R. Chim.* **2015,** *18*, 160-169.
38. Drzewiecki, K. E.; Grisham, D. R.; Parmar, A. S.; Nanda, V.; Shreiber, D. I., Circular Dichroism Spectroscopy of Collagen Fibrillogenesis: A New Use for an Old Technique. *Biophys. J.* **2016,** *111*, 2377-2386.
39. Bruyère, C.; Versaevel, M.; Mohammed, D.; Alaimo, L.; Luciano, M.; Vercruysse, E.; Gabriele, S., Actomyosin contractility scales with myoblast elongation and enhances differentiation through YAP nuclear export. *Sci. Rep.* **2019,** *9*, 15565.
40. Shin, M.; Lee, H. A.; Lee, M.; Shin, Y.; Song, J. J.; Kang, S. W.; Nam, D. H.; Jeon, E. J.; Cho, M.; Do, M.; Park, S.; Lee, M. S.; Jang, J. H.; Cho, S. W.; Kim, K. S.; Lee, H., Targeting protein and peptide therapeutics to the heart via tannic acid modification. *Nat. Biomed. Eng.* **2018,** *2*, 304-317.
41. Evans, N. P.; Call, J. A.; Bassaganya-Riera, J.; Robertson, J. L.; Grange, R. W., Green tea extract decreases muscle pathology and NF-κB immunostaining in regenerating muscle fibers of mdx mice. *Clin. Nutr.* **2010,** *29*, 391-398.
42. Coletti, D.; Teodori, L.; Albertini, M. C.; Rocchi, M.; Pristerà, A.; Fini, M.; Molinaro, M.; Adamo, S., Static magnetic fields enhance skeletal muscle differentiation in vitro by improving myoblast alignment. *Cytometry, Part A* **2007,** *71*, 846-856.
43. Püspöki, Z.; Storath, M.; Sage, D.; Unser, M., Transforms and Operators for Directional Bioimage Analysis: A Survey. In *Focus on Bio-Image Informatics*, De Vos, W. H.; Munck, S.; Timmermans, J.-P., Eds. Springer International Publishing: Cham, 2016; pp 69-93.

Table of contents